On path planning for obstacle avoidance: comparison between two finite element approaches

PAVLOS MAVROMATIDIS[a], ANDREAS KANARACHOS[b]
Electrical Engineering Department[a], Mechanical Engineering Department[b]
Frederick University
7 Y. Frederickou St.
CYPRUS
eng.pam@frederick.ac.cy, eng.ka@frederick.ac.cy http://www.frederick.ac.cy

Abstract: - When an obstacle suddenly appears in the trajectory of a vehicle a path has to be designed in real time to avoid the collision. A vast number of path planning methods for ground vehicles have been proposed until now. A comparative evaluation of the different methods is necessary to illustrate their advantages and disadvantages and ease their selection. In this paper, two different finite element formulations for collision avoidance are presented and compared for a case study, which is used in the literature as a benchmark. Conclusions regarding the performance of the methods are drawn.

Keywords- collision avoidance, path planning, finite elements, dynamics optimization.

1 Introduction

The main cause of road fatalities is human errors in decision making and handling of the vehicle while driving. Further research and development in Advanced Driver Assistance Systems like Lane Keeping and Collision Avoidance Systems has the potential to bring the total number of road fatalities close to zero [1]. A core module for both systems is the path planner. A path has to be designed in real time to avoid the collision and remain within the road boundaries. The path has to be designed in such a way to satisfy vehicle's maneuverability requirements. Although many approaches have been proposed until now there is still lack of a flexible methodology which can satisfy all the above requirements ([2]-[7]).

Gray et al investigated the performance of a point mass path planner and concluded that the trajectory generated, although real-time capable, was not always feasible [8]. The lower level tracking controller could not follow the planned path and obstacle collisions were observed in conditions where the obstacle could have been avoided. Thus, they proposed a path planner based on motion primitives that respect a priori the vehicle dynamics constraints. The main drawback is that motion primitives aren't suitable for complex driving scenarios where arbitrary boundary conditions may hold.

The main reason for which a planned path becomes intractable is because it violates the maneuverability limits of the vehicle. This happens mainly for two reasons (a) the commanded -by the control law- tire forces are too large with respect to the available tire-road friction and/or actuator dynamics and (b) the dynamics of the planned path and the actual vehicle states when path tracking starts have a large discrepancy.

Collision avoidance paths are essentially time optimal two point boundary value problems and thus -from Guidance point of view- should satisfy Pontryagin's Maximum Principle (PMP) [9]. In order to apply the PMP a tire-road friction estimator like the one in [10] is necessary.

Reference [11] has developed, based on PMP, a flexible methodology that could plan obstacle avoidance paths for any vehicle model, however nonlinear it is. The main disadvantage of the method was the computational cost and thus the hardness to meet the real time requirements. In an effort to reduce the computational effort a neural network methodology has been proposed [12]. The neural network was able to plan collision avoidance paths and was real time capable. However, it performed well only in cases for which it has been trained. It was lacking the flexibility to address complex driving scenarios, as one may experience in real life.

In this context, a finite element path planning method which can cope with complex scenarios and arbitrary boundary conditions has been developed

and proposed in [13]. The method decomposes the path in finite standardized segments which are then glued to each other in the same sense as in the direct finite element method. The method can handle complex scenarios and is real time capable.

In this paper, two different formulations of the finite element path planning method are presented and compared. The main driver for it is to evaluate the advantages and disadvantages of each method and thus ease the selection. This work is – to our knowledge- performed for the first time. The rest of the paper is organized as follows: In Sections 2 and 3 the vehicle model used and the finite element formulation which recasts the dynamic optimization problem into a nonlinear algebraic one are discussed respectively. In Section 4 the two finite element formulations are evaluated and compared for different driving scenarios. In Section 5 conclusions and future research directions are drawn.

2 Mathematical model

2.1 Vehicle model and model based constraints

Since a very detailed vehicle model can be difficult to obtain and use, the method described in this paper makes use of a model that approximates vehicle motion. Furthermore, it is assumed that the vehicle is equipped with an Electronic Stability Control (ESC) system, such as the one described in [14]. Furthermore, we assume that the ESC system utilizes the same limit $r_{\max 0}$ as the path tracking system. This effectively means that any commanded yaw rate $r_{des} > r_{\max 0}$ will cause ESC's system activation and thus bring the vehicle from a path tracking to a stability mode.

The two track vehicle model (TTVM), shown in Figure 1, is employed to derive the equations of motion described by forward velocity u_f, lateral velocity v and yaw rate r [15].

For simplification reasons shock absorbers and suspension springs are neglected. Also neglected are roll angle, steer angle and roll axis inclination which are assumed small enough. Effects of additional steer angles due to suspension kinematics and steer compliance are ignored [15]. The equations of motion, Eq. (1)-(3), are:

$$m\cdot\left(\dot{u}_f - r\cdot v\right) = \sum F_x = F_{x1} - F_{y1}\cdot\delta + F_{x2} \tag{1}$$

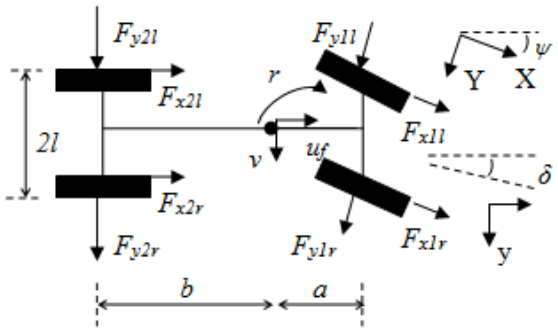

Fig. 1 Top view of TTVM

$$m\cdot\left(\dot{v} + r\cdot u_f\right) = \sum F_y = F_{x1}\cdot\delta + F_{y1} + F_{y2} \tag{2}$$

$$I_z\cdot\dot{r} = \sum M = a\cdot F_{y1} - b\cdot F_{y2} \tag{3}$$

Vehicle velocities and in the global coordinate system O(X,Y) are a function of local velocities and (expressed in the vehicle coordinate system o(x,y) and angle (shown in Figure 1). The vehicle's trajectory (X, Y), expressed in the global coordinate system, is:

$$X = \int_0^T \dot{X}\cdot\cos\psi\cdot dt \tag{4}$$

$$Y = \int_0^T \dot{Y}\cdot\sin\psi\cdot dt \tag{5}$$

where T is the maneuvering time.

Vehicle's yaw rate r is limited either because of the available tire-road friction or because of stability reasons. In the first case, the yaw rate limit $r_{\max 0}$ results from Equation (2):

$$a_y = \dot{v} + u_f\cdot r \approx u_f\cdot r \le a_{y\max} = \mu\cdot m\cdot g \Rightarrow$$

$$r_{\max 0} = \frac{c_0\cdot\mu\cdot m\cdot g}{u_f} \tag{6}$$

where g is the gravitational acceleration and $c_0 \in [0.85, 0.95]$ a coefficient compensating the influence of vehicle slip angle β which is omitted in calculations [16]. In Table 1 the vehicle parameters used in the study are listed.

Table 1 Vehicle parameters.

Name	Parameter	Value
Vehicle mass	m [kg]	1737
Distance from ground to CG	h [m]	0.58
Moment of inertia - to z axis	I_z [kgm^2]	2877
Half length of the wheel axle	l [m]	0.765
Distance of front axle from cog	a [m]	1.3

2.1 Tire model and yaw rate limit

Tire forces are mathematically described using the well-known Magic Formula model. For pure side slip a_s the tire's lateral force F_{y0} is:

$$F_{y0}(\alpha_S) = D \cdot \sin\left(C \cdot \arctan\left(B \cdot \alpha_S - E \cdot \left(B \cdot \alpha_S - \arctan\left(B \cdot \alpha_S\right)\right)\right)\right) \quad (7)$$

where $\alpha_S = \tan(\alpha)$ is the slip angle, $D = \mu \cdot F_z$ the peak value, C the shape factor, $B = \frac{C_{F\alpha}}{C \cdot D}$ the stiffness factor and E the curvature factor. A graphical illustration of lateral force F_y versus slip angle α for four different normal loads is shown in Figure 2. We denote with $\alpha_{\max}(\mu, F_z)$ the tire slip angle for which the lateral force is maximized $F_{y\max}$. In Table 2 the tire parameters used in the study are listed.

Tire slip angles α_1 and α_2 on front and rear wheels are considered small ($\sin\alpha_i \approx \alpha_i$) and expressed as:

$$\alpha_1 = \delta - \frac{1}{u_f} \cdot (v + a \cdot r) \quad (8)$$

$$\alpha_2 = -\frac{1}{u_f} \cdot (v - b \cdot r) \quad (9)$$

where δ is the steer angle. We assume equal slip angles at both left and right wheels ($\alpha_{1r} = \alpha_{1l} = \alpha_1$ and $\alpha_{2r} = \alpha_{2l} = \alpha_2$) which is a valid assumption when $l \cdot |r| << u_f$.

Table 2 Tire parameters.

Name	Parameter	Value
Shape factor	C	1.3
Tire-road friction coefficient	M	0.5
Curvature factor	E	-3
Stifness coefficient	$C_{F\alpha} = c_1 \cdot \sin\left(2 \cdot \arctan\left(\frac{F_z}{c_2}\right)\right)$	
Maximum cornering stiffness [N/rad]	c_1	60000
Load at max. cornering stiffness [N]	c_2	4000

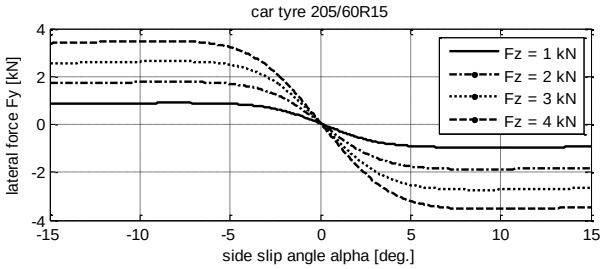

Fig. 2 Lateral force versus tire slip angle for different normal loads

From Equation (8) and (9) and assuming -for simplification reasons - that velocity v is negligible we get respectively:

$$\delta_{\max} = \alpha_{\max} + \frac{1}{u_f} \cdot a \cdot r \quad (10)$$

$$\alpha_{\max} = -\frac{1}{u_f} \cdot \left(v - b \cdot r_{\max_2}\right) \Rightarrow r_{\max 1} = \frac{\alpha_{\max} \cdot u_f}{b} \quad (11)$$

The minimum of yaw rate limits $r_{\max 0}$, and $r_{\max 2}$ is denoted as $r_{\max} = \min(r_{\max 1}, r_{\max 0})$. By implementing a constraint on the maximum yaw rate and maximum tire slip angle we indirectly define a maximum value for the vehicle slip angle.

3 Finite Element Formulation

In this study, two finite element formulations – a third and a second order - are compared. Due to the fact that the first one has been discussed in detail in [13], only the second is presented, in this paper.

3.1 Second order Finite Element Formulation

A schematic of the approach is shown in Figure 3. The total path is decomposed in *N* finite elements/segments. Each finite element is denoted with a number *n=1…N*, and has two nodes: the start node $\mathbf{n}_a$ and end node $\mathbf{n}_b$. The EP is constructed by joining end node $\mathbf{n}_b$ and start node $(\mathbf{n+1})_a$ of two consecutive finite elements **n** and **n+1**, for *n=1:..:N-1*.

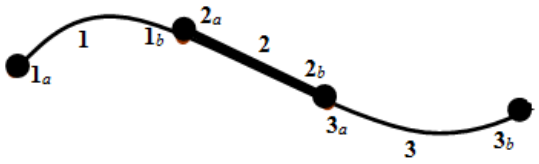

Fig. 3 Collision avoidance path decomposed in 3 finite elements

Each finite element is parameterized using two variables: time span $t_{n\,span}$ and the highest order constrained state variable. Time span $t_{n\,span}$ may be uniformly chosen by decomposing the total maneuvering time in *n* segments or by considering other parameters such as change of tire-road friction coefficient μ and road curvature. In this formulation, angular acceleration is the highest order constrained state variable and assumed constant in each segment for $t_n \in [0, t_{nspan}]$. In this context, angular velocity r_n and position θ_n are:

$$\dot{r}_n = a_{2n} \tag{12}$$

$$r_n = \int_0^{t_{n,span}} \dot{r}_n \cdot dt = a_{2n} \cdot t + a_{1n} \tag{13}$$

$$\theta_n = \int_0^{t_{n,span}} r_n \cdot dt = 0.5 \cdot a_{2n} \cdot t^2 + a_{1n} \cdot t + a_{0n} \tag{14}$$

where $t_n \in [0, t_{nspan}]$.

The states $y_n = \left[\dot{r}_{n,a} \quad r_{n,a} \quad \theta_{n,a} \quad \dot{r}_{n,b} \quad r_{n,b} \quad \theta_{n,b}\right]^T$ at the boundaries of the finite element are expressed in matrix form as:

$$\mathbf{y_n} = \mathbf{A_n} \cdot \mathbf{x_n} \tag{15}$$

$$\mathbf{y_n} = \left[\, r_{n,a} \quad \theta_{n,a} \quad r_{n,b} \quad \theta_{n,b}\right]^T \tag{16}$$

$$\mathbf{x_n} = \left[\, a_{2n} \quad a_{1n} \quad a_{0n}\right]^T \tag{17}$$

$$\mathbf{A}_n = \begin{bmatrix} 0 & 1 & 0 \\ 0 & 0 & 1 \\ t_{nspan} & 1 & 0 \\ 0.5 \cdot t_{nspan}^2 & t_{nspan} & 1 \end{bmatrix} \tag{18}$$

The finite element matrix A_n constitutes the basis for joining subsequent elements and deriving the system's solution. For a detailed description the reader is referred to [13].

3.2 Solution methodology

The path is decomposed in N=3 uniform finite elements with the same time span . The EP is computed by solving the following linear system of equations:

$$\mathbf{y}_{bc} = \mathbf{A} \cdot \mathbf{x}_u \tag{19}$$

$$\mathbf{y}_{bc} = \left[r_{1,ades} \quad \theta_{1,ades} \quad \ldots \quad r_{n,bdes} \quad \theta_{n,bdes}\right]$$

$$\mathbf{x}_u = \left[a_{21} \quad a_{11} \quad a_{01} \quad \ldots \quad a_{2n} \quad a_{1n} \quad a_{0n}\right]$$

$$\sum_{i=1}^{N} t_{nspan} = T$$

where $\mathbf{y}_{bc}$ is the vector of boundary conditions, $\mathbf{x}_u$ is the vector of unknown coefficients and **A** the system's matrix.

Vectors $\mathbf{x}_u$ and $\mathbf{y}_{bc}$ as well as system matrix **A** are formed by joining subsequent elements. In particular, we use the desired conditions at beginning (*t=0*) and end (*t=T*) of the EP:

- $r(t=0) = r_{1,ades}$ and $\theta(t=0) = \theta_{1,ades}$
- $r(t=T) = r_{N,bdes}$ and $\theta(t=T) = \theta_{N,bdes}$

To assemble system matrix **A** we use the continuity equations between subsequent elements

$$r_{n,b} = r_{n+1,a}, \theta_{n,b} = \theta_{n+1,a} \tag{20}$$

and the desired lateral displacement Y_{des} at the end (*t=T*) of the EP:

$$\sum \delta Y_n = Y_{des} \tag{21}$$

where δY_n is the lateral displacement of a finite element:

$$\delta Y_n = \int_0^{t_n t_{span}} u_f \cdot \sin(\theta_n) \cdot dt \approx u_f \cdot \int_0^{t_n t_{span}} \theta_n \cdot dt = \left(\frac{1}{6} \cdot \alpha_{2n} \cdot t_n^3 + \frac{1}{2} \cdot \alpha_{1n} \cdot t_n^2 + \alpha_{0n} \cdot t_n \right) \cdot u_f \tag{22}$$

In Equation (22) the incremental lateral displacement δY_n is linearized by assuming $\sin(\theta_n) \approx \theta_n$. The proposition is valid only for small angles $\theta_n \leq 5^o$. For larger angular displacement θ_n the path has to be decomposed into a greater number of finite elements.

It is obvious that different path decomposition would lead to a different system matrix **A** and subsequently a different solution. Actually, there are infinite EPs that satisfy the boundary conditions and that can be computed using the FE method. This is exactly the reason why we are interested in comparing the two different formulations.

4 Numerical results

The finite element formulations have been tested for an extensive number of driving scenarios in Matlab simulation environment. The numerical examples are based on the vehicle data listed in Table 1 and tire parameters listed in Table 2. One driving scenario which highlights their features is presented and discussed.

In the scenario considered it is assumed that the vehicle moves in a straight line road segment with a speed $u_f = 30\, m/s$. The road surface is dry $\mu = 1$ and an obstacle at distance $d = 54\, m$ suddenly appears in its direction of travel. To avoid the collision the vehicle has to displace laterally by $Y_{des} = 3\, m$.

We solve the problem by decomposing the path in uniform road segments and apply the solution methodology described in the previous section and in [13]. The numerical results using the second order finite element methods are shown in Figs 4-6, while those with the 3rd order method in Figs 7-9.

5 Conclusions

When an obstacle suddenly appears in the trajectory of a vehicle a path has to be designed in real time to avoid the collision. A vast number of path planning methods for ground vehicles have been proposed until now. A comparative evaluation of the different methods is necessary to illustrate their advantages and disadvantages and ease their selection. In this paper, two different finite element formulations for collision avoidance are presented and compared for a case study.

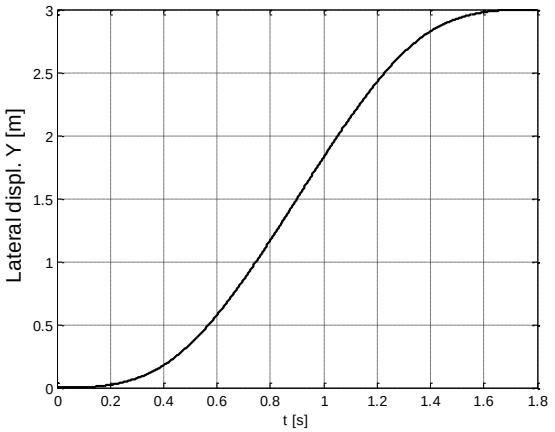

Fig. 4 Lateral displacement using the 2nd order FE method

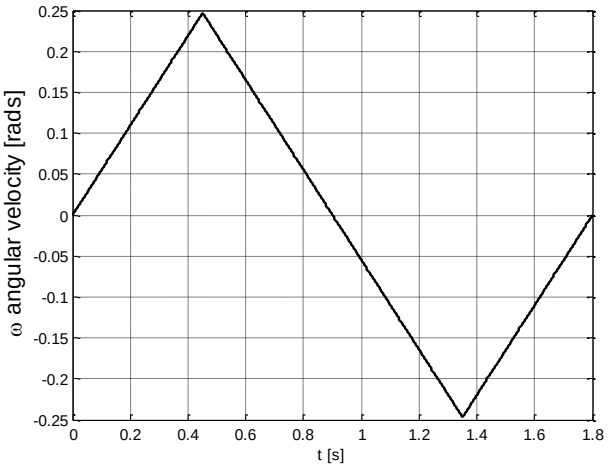

Fig. 5 Angular velocity using the 2nd order FE method

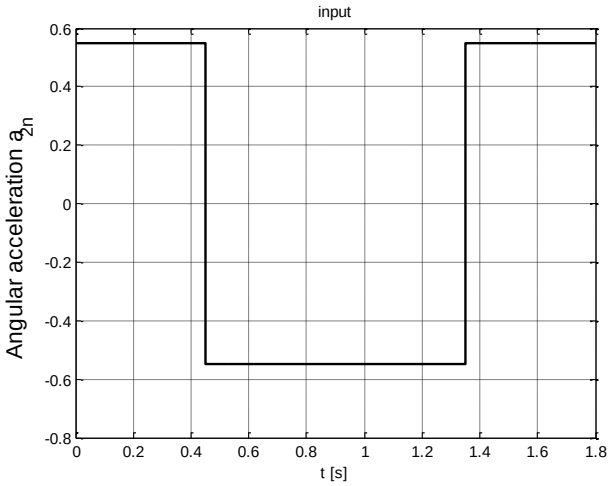

Fig. 6 Angular acceleration using the 2nd order FE method

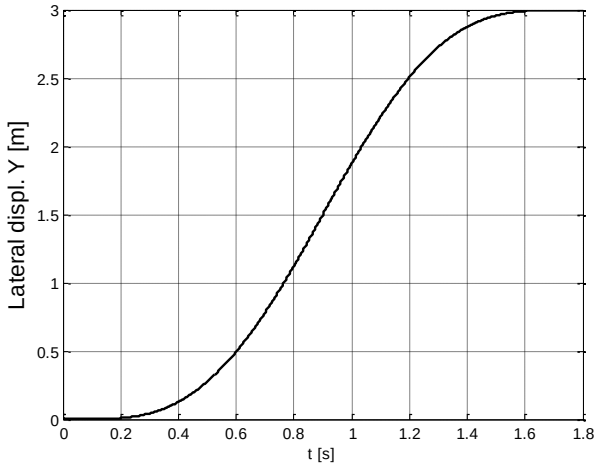

Fig. 7 Lateral displacement using the 3rd order FE method

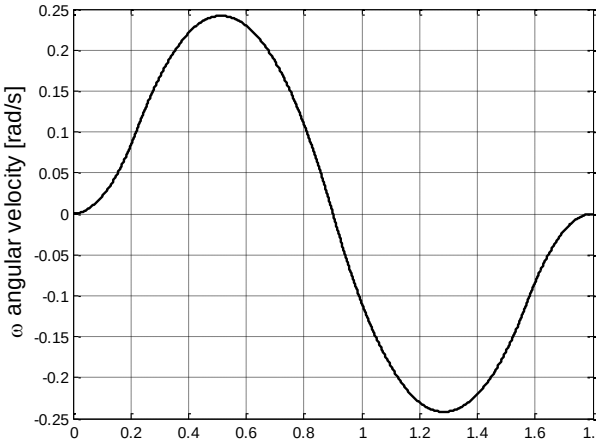

Fig. 8 Angular velocity using the 3rd order FE method

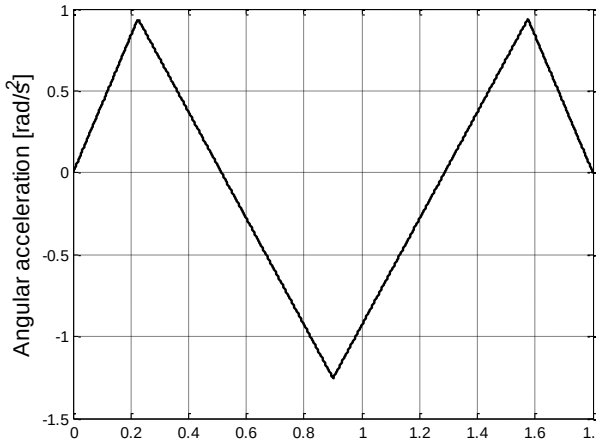

Fig. 9 Angular acceleration using the 3rd order FE method

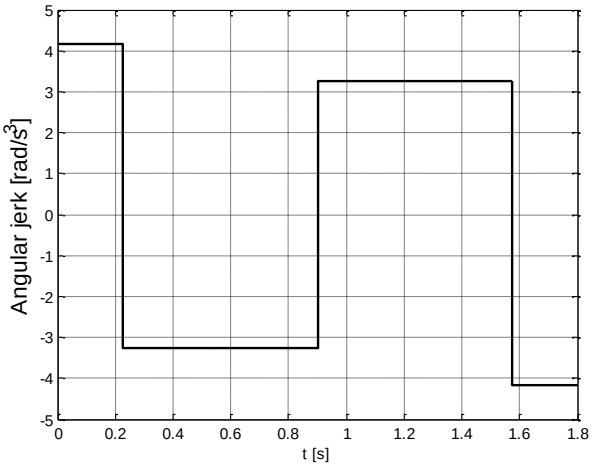

Fig. 10 Angular jerk using the 3rd order FE method

A finite element (FE) method has been developed based on a reformulation of Pontryagin's Maximum Principle to plan collision avoidance-time optimal paths. Two different formulations, which differ in the order of approximation, have been presented and evaluated in this study for a typical collision avoidance scenario.

From the numerical results it becomes clear that both methods a) improve the path dynamics compared to the solution obtained with a uniform time mesh and b) satisfy the maneuverability requirements of the vehicle with respect to the maximum admissible yaw rate However, the methods differ in the achievable maximum acceleration and maximum jerk. In the 2nd order method the maximum acceleration is smaller (44%) compared to the one obtained with the 3rd order method. However, the angular jerk is infinite which is negative in terms of comfort. Furthermore, if an active steering system is used to guide the vehicle it is a wrong assumption since the steering dynamics isn't negligible. In case a differential braking system is used then it is an acceptable solution.

In the future the design of collision avoidance paths should become standard and available through the communication protocols between vehicles. The development of a simple but powerful method like the one presented in this paper is considered to be a contribution in this direction.

References:

[1] Sotelo Miguel, Advanced Techniques for Vision-based Pedestrian Recognition, *Proceeding VIS'08 Proceedings of the 1st*

WSEAS international conference on Visualization, imaging and simulation , 2008.

[2] Wan Ngah, W.A.J., Buniyamin N, Mohamad Z. Point to Point Sensor Based Path Planning Algorithm for Mobile Robots. in *9th WSEAS International Conference on System Science and Simulation in Engineering (ICOSSSE'10)*. 2010. Iwate, Japan: WSEAS.

[3] Vacariu, L., Flaviu Roman, Mihai Timar,Tudor Stanciu, Radu Banabic, Octavian Cret. Mobile Robot Path-planning Implementation in Software and Hardware. *in 6th WSEAS International Conference on Signal Processing, Robotics and Automation*. 2007. Corfu Island, Greece.

[4] Sariff, N., Buniyamin N. Ant Colony System For Robot Path Planning In Global Static Environment. *in 9th WSEAS International Conference on System Science and Simulation in Engineering (ICOSSSE'10),*. 2010. 4th -6th October, Iwate, Japan: WSEAS Pres

[5] Glavaski, D., Volf M., Bonkovic M., Mobile robot path planning using exact cell decomposition and potential field methods. *WSEAS Transactions on Circuits and Systems* 2009. 8(9).

[6] Xiao-Guang, G., Xiao-Wei Fu,Da-Qing Chen. Genetic-Algorithm-Based Approach to UAV Path Planning Problem. *in 5th WSEAS Int. Conf. on SIMULATION, MODELING AND OPTIMIZATION*, 2005. Corfu, Greece.

[7] Susnea, I., Viorel Minzu, Grigore Vasiliu. Simple, real-time obstacle avoidance algorithm for mobile robots. in *8th WSEAS International Conference on Computational intelligence, man-machine systems and cybernetics* (CIMMACS'09) 2009.

[8] Gray, A., Yiqi Gao, Lin, T., Hedrick, J.K., Tseng, H.E., Borrelli, F. (2012) 'Predictive control for agile semi-autonomous ground vehicles using motion primitives', *Proceedings of the American Control Conference* 2012, pp. 4239-4244, 27-29 June 2012.

[9] Kanarachos, S., Koulocheris, D., Spentzas, C., Optimal open loop control of dynamic systems using a "min-max" Hamiltonian method, *Forschung im Ingenieurwesen/Engineering Research*, 69 (1), 2004, pp. 1-10.

[10] Valentin Ivanov, Barys Shyrokau, Klaus Augsburg, Vladimir Algin, Fuzzy evaluation of tyre–surface interaction parameters, *Journal of Terramechanics*, Volume 47, Issue 2, April 2010, pp. 113-130.

[11] Kanarachos, S.A., A new method for computing optimal obstacle avoidance steering manoeuvres of vehicles, *International Journal of Vehicle Autonomous Systems*, 7 (1-2), 2009 pp. 73-95.

[12] Kanarachos, S. Design of an intelligent feed forward controller system for vehicle obstacle avoidance using neural networks, *International Journal of Vehicle Systems Modelling and Testing*, 8 (1), 2013, pp. 55-87.

[13] Kanarachos, S., Alirezaei M., An adaptive finite element method for computing emergency maneuvers of ground vehicles in complex driving scenario- Accepted for publication, *International Journal of Vehicle Systems Modelling and Testing*, to be published.

[14] Kanarachos, S., Alirezaei, M., Jansen, S., Maurice, J.-P., Control allocation for regenerative braking of electric vehicles with an electric motor at the front axle using the state-dependent Riccati equation control technique, Proceedings of the Institution of Mechanical Engineers, Part D: Journal of Automobile Engineering, 228 (2), (2014) pp. 129-143.

[15] Pacejka, B., *Tire and Vehicle Dynamics*, Chapter 1, Society of Automotive Engineers, Warrendale. 2005.

[16] R. Rajamani, Vehicle Dynamics and Control - Chapter 8: Electronic Stability Control, Springer, New York, 2012